

Modelling of Fracture Initiation and Post-Fracture Behaviour of Head Impact on Car Windshields

Karoline Osnes¹, Sebastian Kreissl², Jonas D'Haen², Tore Børvik¹

¹Structural Impact Laboratory (SIMLab), Department of Structural Engineering, NTNU – Norwegian University of Science and Technology, Trondheim, Norway

²BMW Group Research and Innovation Center FIZ, Munich, Germany

1 Introduction

More than half of all road fatalities involve vulnerable road users, such as pedestrians and cyclists [1]. When involved in crashes with cars, the head is particularly susceptible to injuries, and especially if the road user hits the windshield of the car [2]. Impact tests are often performed to estimate the risk of head injury during such an event. A pedestrian head strike test normally involves a spherical headform, in which the likelihood of head injury is described by the head injury criterion (HIC) [3]. The HIC value is based on the mean value of the acceleration over the most critical stage of the head's motion, and is calculated as

$$\text{HIC} = \max_{t_1, t_2} \left\{ (t_2 - t_1) \left[\frac{1}{t_2 - t_1} \int_{t_1}^{t_2} a(t) dt \right]^{2.5} \right\}$$

Here, $a(t)$ is the acceleration of the head, and t_1 and t_2 denote the start and the end of the most critical stage, respectively. For the head impact on the front of the vehicle the duration $t_2 - t_1$ is generally limited to 15ms. In this study, we aim to recreate the acceleration-time history (and thus the HIC value) of a headform during two preliminary impact tests on windshields through finite element (FE) simulations in LS-DYNA. The impact tests were performed at BMW's research and innovation centre in Munich, Germany, in 2019.

2 Experiments

In the impact tests, the headform was launched towards the left side of the windshields at a velocity of 35 km/h and an angle of 65 degrees (relative to the road). See Figure 1 for an illustration of the setup. To protect the headform from potential glass shards, a rubber foam disc was placed on the windshield at the impact point. The influence of the foam disc on the acceleration history is assumed to be small. Note that later tests will follow the EURO NCAP protocol [4], thus excluding the foam disc and performing the tests at 40km/h. The investigated windshields consist of two layers of glass and a polymer interlayer made from polyvinyl-butylal (PVB). The weight of the headform is 4.5 kg and comprises of a metal sphere, -plates, -bolts, and a polymer skin layer. It also contains an accelerometer for acceleration-time measurements.

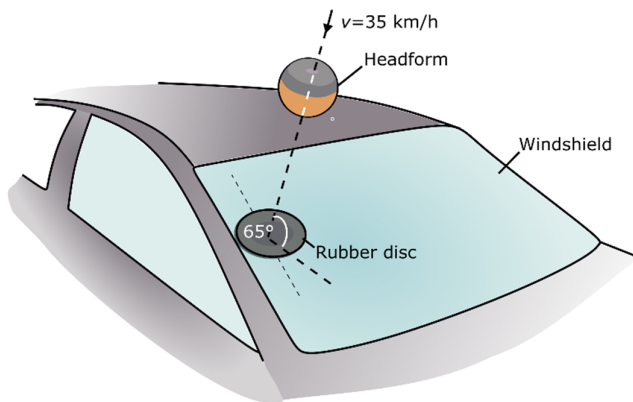


Fig.1: Setup of the impact tests

The resulting acceleration-time history of the headform during the two impact tests are presented in Figure 2a, while Figure 2b denotes three different stages during the loading of the windshield. The three stages are as follows: (1) pre-fracture, (2) fracture in the first glass layer while the second layer is still intact, and (3) post-fracture. In the last stage, the PVB is activated and undergoes large deformations, which leads to a significant amount of energy absorption. Please note that the acceleration data are confidential, and the values on the ordinate are therefore given as products of a scalar α .

From Figure 2a, it becomes apparent that the acceleration-time curve is dependent on the time of fracture initiation in the glass layers. This time difference arises from the fact that glass has a probabilistic fracture strength, which results from inherent microscopic surface flaws [5][6]. For test 1, fracture initiation occurred in the inner glass layer at $t = 1.85$ ms and in the outer glass layer at 2.55 ms. Fracture initiation occurred slightly earlier for test 2, i.e., at $t = 1.25$ ms and $t = 2.05$ ms for the inner and outer glass layer, respectively. Consequently, the PVB was activated earlier in test 2 compared to test 1. The calculated HIC values for tests 1 and 2 were $17.8\alpha^{2.5}$ and $15.7\alpha^{2.5}$. Generally, early fracture initiation yields a higher HIC value. However, the adhesive that connects the windshield to the car frame suffered some damage close to the impact point in test 2. This might explain the irregular shape of the PVB activation stage for test 2 (Figure 2a), and why the HIC value was lower for test 2 compared to test 1.

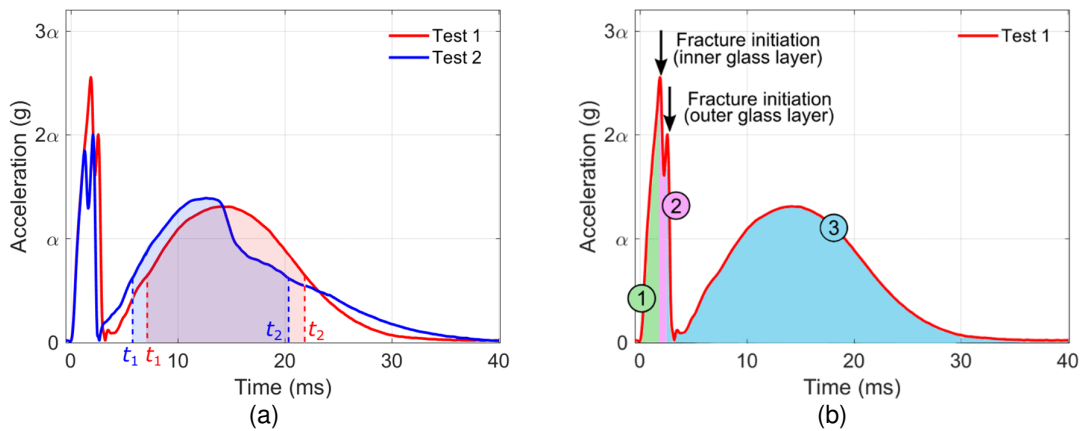


Fig.2: Experimental results of the impact tests: a) acceleration-time curves with denoted critical area (t_2-t_1) for the HIC value, and b) different stages of the impact test

The fracture pattern of the windshield in test 1 after loading is presented in Figure 3. It consists of both circumferential and radial cracks, and the crack density gets larger closer to the impact point. The fracture pattern for test 2 is highly similar, however, the cracks in test 2 cover a slightly larger area.

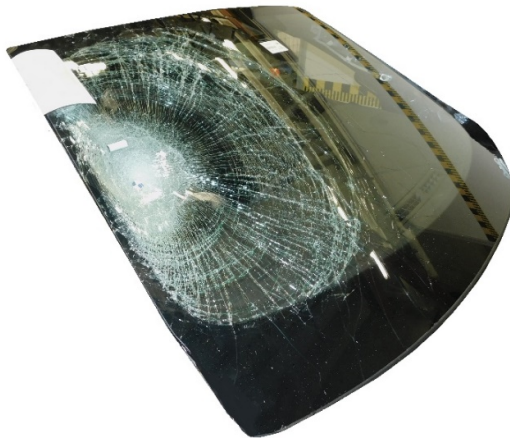


Fig.3: Fractured windshield after impact test 1 (other car parts are excluded from the image)

3 Numerical modelling

3.1 LS-DYNA simulations

For the simulations of the head impact tests, we used LS-DYNA version R12. To save computational cost, the FE model of the car was reduced to the relevant components, i.e., the windshield and the frame, and some surrounding components. The windshield was glued to the frame, and the adhesive was described by cohesive elements. The windshield was discretised by shell elements for the glass layers and solid elements for the PVB interlayer. The glass and PVB layers were tied together by shared nodes, and the in-plane mesh size was approximately 8 mm × 8 mm. The PVB material was described by ***MAT_PIECEWISE_LINEAR_PLASTICITY** (***MAT_24**) with strain rate dependency, while ***MAT_GLASS** (***MAT_280**) was used to model the glass [7]. The ***MAT_GLASS** model describes a material by linear elasticity with a stress-based failure criterion (with tension-compression asymmetry). Failure (or glass fracture) is treated without element erosion and is instead described by reducing the stiffness and stresses in the failed elements. Consequently, the laminated glass can still carry compressive loads after glass fracture. Another useful feature of ***MAT_GLASS** is the parameter FTSCCL. When the maximum principal stress σ_1 equals the tensile strength (FT) in an element, it will fail. However, if $FTSCCL \geq 1.0$, fracture initiation (failure in the first element) in a part occurs at $FTSCCL \times FT$. After fracture initiation, the remaining elements in the part will fail at FT. In this study, we made use of the FTSCCL parameter to capture the high stresses necessary to initiate fracture at the correct time, and to recreate the rapid crack growth in glass. The fracture stress parameters (FT × FTSCCL) in ***MAT_GLASS** were chosen through a reverse-engineering approach such that the fracture initiation times corresponded with the tests. Table 1 presents the fracture stress parameters used for the two glass layers in the two tests. The parameter FT = 60 MPa was chosen through preliminary numerical studies as it agreed well with experimental tests. The remaining parameter input for ***MAT_GLASS** is presented in Table 2.

| Test number | FTSCCL × FT (inner) | FTSCCL × FT (outer) |
|-------------|------------------------|------------------------|
| 1 | 6.9 × 60 MPa = 414 MPa | 8.6 × 60 MPa = 516 MPa |
| 2 | 5.1 × 60 MPa = 306 MPa | 8.0 × 60 MPa = 480 MPa |

Table 1: Fracture stress input in ***MAT_GLASS**

| | | |
|-------|---|-------------|
| RO | Density (kg/m ³) | 2500 |
| E | Young's modulus (MPa) | 70000 |
| PR | Poisson's ratio | 0.23 |
| FT | Tensile strength (MPa) | 60 |
| FC | Compressive strength (MPa) | 1200 |
| FTSCL | Scale factor for the tensile strength | See Table 1 |
| SFSTI | Scale factor for the stiffness after failure | 0.001 |
| SFSTR | Scale factor for the stress after failure | 0.01 |
| ECRCL | Strain to reopen cracks | 0.0 |
| NCYCR | Number of cycles to reduce the stress | 100 |
| NIPF | Number of integration points to fail an element | 1 |

Table 2: Parameter input for ***MAT_GLASS**

The results from the numerical simulations of tests 1 and 2 are presented in Figures 4 and 5. The initial acceleration tops with a subsequent drop before the PVB-activation stage are captured accurately. The duration of the PVB-activation stage also corresponds well with the tests. However, the accelerations in the simulations exceed the tests' by about 40 % at around $t = 15$ ms. It should be noted that modifying the ***MAT_GLASS** parameters did not improve these results. Thus, the material model of the PVB was considered the most likely cause of the discrepancy. Note also that the shape of the acceleration-time curve of test 2 was not properly recreated, probably because the adhesive failure was not captured in the simulation. Figures 4b and 5b present the fracture pattern of the windshields after impact (at $t = 35$ ms). The history variable (ranging here from 0 to 2) shows the number of cracks caused by tensile failure and represent in some way the severity of damage in the glass. A value of -1 is possible, and represents compressive failure, however, this did not occur in these simulations. The comparison between the simulations and the test (Figure 3) shows good agreement regarding the fracture pattern, both in terms of the area covered by cracks, and the shape and general appearance of the fracture patterns.

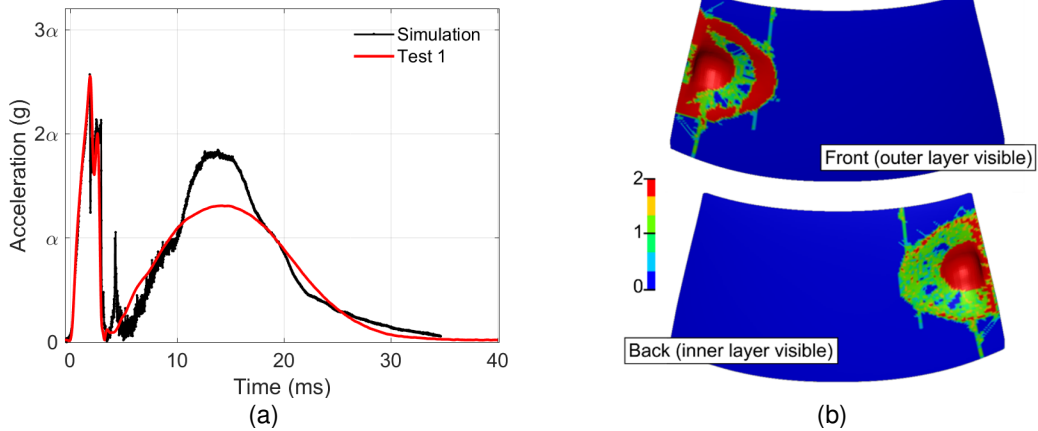


Fig.4: Results from the numerical simulation of test 1: a) acceleration-time history (test results included), b) fracture pattern (history variable shows “number of cracks”) at $t = 35$ ms

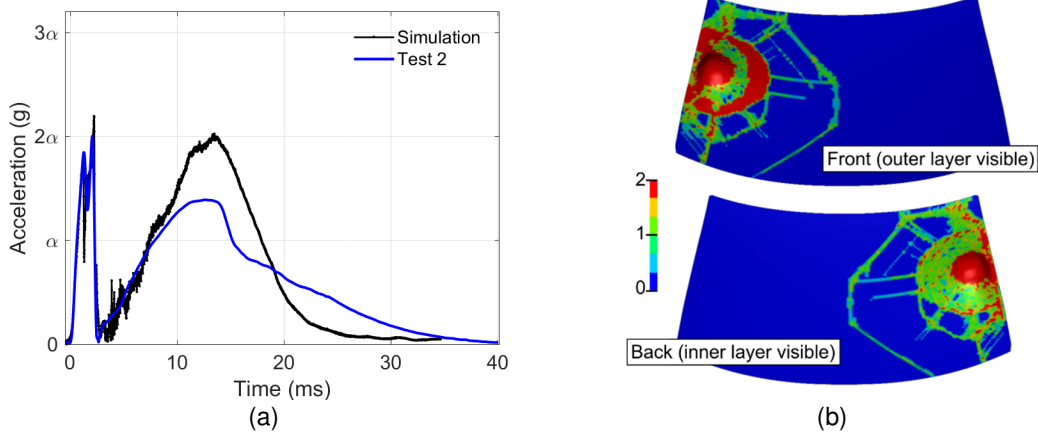


Fig.5: Results from the numerical simulation of test 2: a) acceleration-time history (test results included), b) fracture pattern (history variable shows “number of cracks”) at $t = 35$ ms

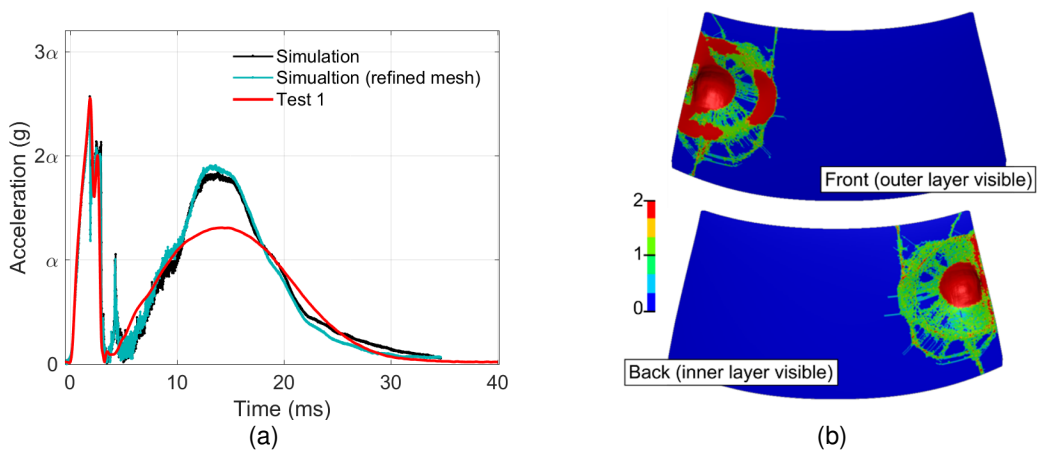


Fig.6: Results from the numerical simulation with a refined mesh ($4\text{ mm} \times 4\text{ mm}$): a) acceleration-time histories b) fracture pattern (history variable shows “number of cracks”) at $t = 35$ ms

We also run an additional simulation of test 1 to study the mesh sensitivity. The elements of the windshield were reduced to 4 mm × 4 mm, and the FTSCl was increased with 0.2 to achieve fracture initiation at the same time as before. The acceleration-time histories for the original and refined models are compared in Figure 6a and show only minor differences. Figure 6b presents the fracture pattern and demonstrates that the refined mesh might produce slightly more realistic cracking than the original mesh. However, the changes are not substantial.

| | Physical tests | | Simulation | | Simulation (refined) | |
|---------------|--------------------|----------------------------|--------------------|----------------------------|----------------------|----------------------------|
| | HIC | $t_1 \rightarrow t_2$ (ms) | HIC | $t_1 \rightarrow t_2$ (ms) | HIC | $t_1 \rightarrow t_2$ (ms) |
| Test 1 | $17.8\alpha^{2.5}$ | 7.2 → 21.9 | $25.6\alpha^{2.5}$ | 8.6 → 20.1 | $27.7\alpha^{2.5}$ | 8.4 → 19.6 |
| Test 2 | $15.7\alpha^{2.5}$ | 5.8 → 20.4 | $32.1\alpha^{2.5}$ | 7.2 → 18.2 | | |

Table 3: HIC values for the tests and simulations

Table 3 gives an overview of all calculated HIC values and shows a considerable difference between the values of the tests and the simulations. The deviation is mainly caused by the PVB activation stage and requires a closer investigation of the PVB material model. The table also illustrates that the HIC value is sensitive to small changes in the acceleration history, as the refined mesh increased the HIC value with 8 %.

3.2 Fracture strength prediction

The numerical work presented in Section 3.1 demonstrates that the first stages of the impact loading can be captured accurately if fracture is initiated at the correct time. However, the fracture stresses (controlled by the scale factor FTSCl) were chosen to match the fracture initiation in the individual tests. For designing windshields, this is a costly and impractical process. An alternative solution is to find the probability distribution of the glass' fracture stress by numerical calculations.

In this study, we aimed to find this probability distribution by employing a “strength prediction model” developed by two of the current authors [5][6]. The probabilistic fracture strength of glass originates from microscopic surface flaws, in which fracture generally initiates. The “strength prediction model” is based on this failure mechanism and the theory of linear elastic fracture mechanics. Due to the nature of these flaws, the probabilistic fracture strength will depend on a glass plate's dimensions and shape, the boundary and loading conditions, and the loading rate. To get a proper distribution of the fracture strength of a setup, a “strength prediction” analysis consists typically of 5000 virtual experiments. The parameter input is presented in Table 4. Please refer to Osnes et al. [4][5] for a thorough description of the model and definitions of the parameters.

| | | | | |
|-----------|-----------------------|-------|------------------|------------------|
| a_{max} | ρ_{flaw} | N_s | ϵ_0 | t_c |
| 0.75 mm | 1/128 mm ² | 12.0 | 10 ⁻⁵ | 10 ⁻⁴ |

Table 4: Input parameters of the “strength prediction model”, see [5] and [6] for a description.

The results from the “strength prediction” analysis of the head impact setup are presented in Figure 7. Figure 7a presents the predicted fracture initiation time and fracture stress by boxplots. The box contains 50 % of the results, the line inside the box denotes the median, and the grey plus signs depict the cases outside the 1st and 99th percentile. The red and blue arrows indicate the values associated with tests 1 and 2, respectively. Both fracture times and the fracture stress for test 2 fall very well within the distributions, while the fracture stress for test 1 is almost on the limit of the 99th percentile. This might indicate that the predicted stress distribution is slightly skewed, however, more validation is needed to make any definite conclusions. Furthermore, Figure 7b illustrates the predicted positions of fracture initiation (with denoted failure percentage). Due to the microscopic surface flaws, glass fracture does not necessarily initiate at the position of maximum principal stress; however, for this setup, fracture will initiate very close to the impact point and the maximum principal stress. The analysis also predicted failure in all 5000 virtual experiments, and in 99.99 % of the cases, initiation occurred in the inner glass layer.

Please note that these “strength prediction” results represent fracture initiation only in the first glass layer. To employ the “strength prediction model” to predict fracture in the second glass layer (in the second stage) poses additional challenges and will be a topic for further work. At present, the model can still be used to indicate when the first glass layer fractures. It can further be assumed that fracture

in the second layer follows the first one shortly after. In that way, the “strength prediction model” can be a helpful design tool for the head impact test.

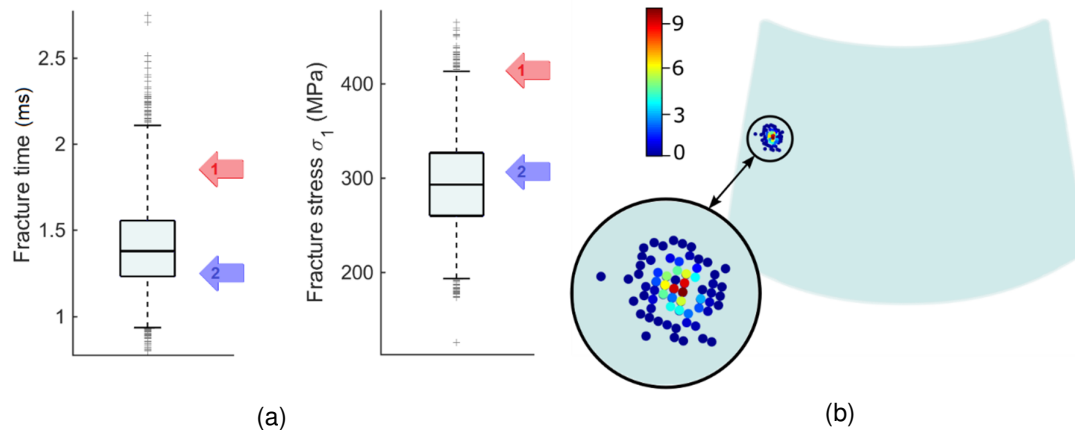


Fig.7: Results from the “strength prediction model”: a) predicted fracture time and stress with arrows denoting test values, b) predicted positions of fracture initiation (legend: failure percentage)

4 Summary

The objective of this study was to recreate the acceleration-time history (and the HIC value) of two impact tests on windshields through FE simulations in LS-DYNA. The material model ***MAT_GLASS** was used to describe the glass material in the windshield, while the PVB interlayer was modelled by ***MAT_PIECEWISE_LINEAR_PLASTICITY**. In order to capture the first stages (glass fracture) of the impact loading, it was crucial to predict the correct fracture initiation points, in addition to a rapid fracture propagation in the glass. This was enabled by the scale factor FTSCl in ***MAT_GLASS**. The initial fracture stress values (FT \times FTSCl) were chosen through a reverse-engineering approach. The simulations corresponded well with the experiments; however, the accelerations overshoot with about 40 % during parts of the PVB activation stage.

Glass has a stochastic fracture behaviour, which complicates the choice of fracture stresses in the FE simulations. To estimate the variation in the fracture stress (and fracture time) for the current test setup, we employed an earlier presented “strength prediction model”. For the two considered impact tests, the predicted fracture initiation stress and time for the inner glass layer corresponded well with the physical tests.

5 Acknowledgement

The present work has been carried out with financial support from the Centre of Advanced Structural Analysis (CASA), Centre for Research-based Innovation, at the Norwegian University of Science and Technology (NTNU) and the Research Council of Norway through project no. 237885 (CASA).

6 Literature

- [1] World Health Organization: “Road traffic injuries” <https://www.who.int/news-room/fact-sheets/detail/road-traffic-injuries>, 2021
- [2] Otte D., Jänsch M., Haasper C.: “Injury protection and accident causation parameters for vulnerable road users based on German In-Depth Accident Study GIDAS”. Accident Analysis & Prevention 44, 2012, 149-53
- [3] Wikipedia: “Head injury criterion” https://en.wikipedia.org/wiki/Head_injury_criterion, 2021
- [4] Euro NCAP: “Vulnerable Road User (VRU) Protection: Head impact” <https://www.euroncap.com/en/vehicle-safety/the-ratings-explained/vulnerable-road-user-vru-protection/head-impact/> 2013.
- [5] Osnes K., Børvik T., Hopperstad O.S.: “Testing and modelling of annealed float glass under quasi-static and dynamic loading”. Engineering Fracture Mechanics 201, 2018, 107-129

- [6] Osnes K., Hopperstad O.S., Børvik T.: "Rate dependent fracture of monolithic and laminated glass: Experiments and simulations". Engineering Structures 212, 2020, 110516
- [7] Livermore Software Technology Corporation. "LS-DYNA keyword user's manual. Volume II: Material Models" r:13191, 2020